On the inner structure of streamwise Görtler rolls

H. Peerhossaini and J. E. Wesfreid
Laboratoire d'Hydrodynamique et Mécanique Physique, U.A. 857-CNRS, ESPCI,
10 rue Vauquelin, 75231 Paris Cedex 5, France

Received 14 November 1986 and accepted for publication on 13 April 1987

Counterrotating streamwise rolls are generated on a concave wall due to Görtler instability mechanism and are studied as they emerge into a stragiht after-section where the destabilizing mechanism is relaxed. Once the Görtler rolls develop, increasing the Görtler number causes the center of the rolls to move off the wall. At higher Görtler numbers, a higher mode of instability sets in, which appears as side oscillations of the interface plane between two neighboring rolls. Amplified oscillations bend the rolls drastically so that their centers move close to the wall. A higher mode of instability can be obtained at higher Görtler numbers. This mode is characterized by lateral wandering of the rolls. Eventually when the boundary layer becomes turbulent, the distorted rolls still keep their intermittent presence.

Keywords: Görtler vortex; concave boundary layers; centrifugal instabilities; hydrodynamic instabilities

Introduction

The influence of counterrotating Görtler rolls on local heat, mass, and momentum transfer from a wall has been examined experimentally. Streamwise rolls can lead to up to 80% enhancement in local heat transfer from the wall.[1] Even enhancements of the order of 100% to 150% in heat transfer due to the rolls have been reported in the literature.[2] However, a reliable model for calculating transfer phenomena close to a concave wall suffers from lack of knowledge on basic characteristics of the Görtler rolls.

Streamwise Görtler rolls may develop in a concave boundary layer owing to centrifugal instability. The corresponding control parameter for this instability is the Görtler number defined as

$$G_\theta = \left(\frac{U\theta}{\nu}\right)\left(\frac{\theta}{R}\right)^{1/2} \tag{1}$$

where U, θ, ν, and R represent freestream velocity, momentum thickness, kinematic viscosity, and radius of curvature, respectively.

Roll characteristics such as the threshold of appearance, sensitivity to upstream fluctuations, wavelength selection mechanism, dynamics, and more generally, the inner structure of the rolls are either controversial or partly unknown.[3,4] The available experimental results suggest, on the one hand, the rolls' wavelengths observed in experimental apparatus either are intentionally imposed by perturbing devices such as wings,[5] heating elements,[6] and grids[1] or, indirectly, are induced by honey combs and grids in the settling chamber or by the concavity of nozzles. Kottke[1] has stated that without a grid in front of his concave test section, no appreciable streamwise roll can be generated. Swearingen and Blackwelder[7] have demonstrated the prevailing wavelength of the rolls can be changed simply by changing the mesh size of grid sets in the settling chamber.

On the other hand, closely observing the Görtler rolls reveals each low-speed streak between two adjacent rolls (upflow interface) may break independently. This work was prompted by these observations and by a need for further information on the inner structure of the Görtler streamwise rolls. The results of this investigation can contribute to a better understanding of local transfer phenomena between a fluid and a solid wall due to the presence of streamwise rolls.

Experimental arrangement and methods

The experiments were carried out in a low-speed, open-return water tunnel. The tunnel was especially designed so that the laminar boundary layers on the test section would start to develop from the concave surface leading edge and would become unstable to a Görtler instability earlier than the Tollmien-Schlichting instability. The width and height of the tunnel at the test section are 10 and 5 cm, respectively, and the radius of curvature R of the test section is 10 cm. Flow is generated from a constant level reservoir. The streamwise velocity component is measured by laser Doppler anemometry, and the experiments were conducted at velocities ranging from 2 to 8 cm/s. However, higher velocities in the tunnel are easily attainable.

The boundary layers developed upstream of the test section are eliminated at the entry to the test section through four suction slots, one for each side. The suction rate at each slot is controlled by independent valves to obtain the desirable flow in the test section.

The freestream velocity fluctuation intensity in the streamwise direction at the test-section entry was typically 1.9% for the range of the velocities used in the experiment. The intensity of velocity fluctuation in the normal to the wall direction at the same point was between 0.5% and 0.8%. These values were obtained from the contribution of velocity fluctuations to the broadening of the Doppler spectra.

Details of the tunnel design and its specifications have been already reported in Peerhossaini *et al.*[8] Figure 1(a) shows schematically the water tunnel.

For flow visualization, the experimental apparatus is equipped with two dye injection facilities, namely, wall injection and bulk injection. In the wall injection technique, dye is

introduced beneath the boundary layer on the concave wall through porous metal strips 0.4 cm wide that span the test section and are located at 11° and 64° from the leading edge. The dye so introduced forms a very thin colored film adjacent to the concave wall and is brought to a streamwise streak pattern downstream owing to the vortex action. In the bulk injection technique, dye is introduced into the bulk flow at the entry to the tunnel. From the injection point up to the inlet of the test section, dye mixes partly with the working fluid. Dye-marked streamlines are then brought to a rotating motion in the test section owing to the destabilizing mechanism. In this manner, the gradient of dye concentration inside the Görtler rolls reveals their inner structure.

The dye used for visualizing the flow is fluorescein sodium salt ($C_{20}H_{10}O_5Na_2$) diluted in water to 0.1 grams per liter. The chemical is very soluble in water, and the strength of the solution required is so diluted that the difference in density between the dye and water is negligible. The injected dye has the same temperature as the working fluid. In room light, the solution is a yellowish liquid. Molecules of dye can be excited by blue light, and then they emit green light. For the fluorescein used in our experiment, excitation occurs under incident blue light of 491 nm wavelength. When the dye is excited, maximum emission occurs at green light of 514 nm wavelength. We used an argon ion laser of low power (40 mW) to excite the fluorescein. The laser beam was directed through a cylindrical lens and expanded into a thin sheet of light. The light sheet was then directed through the flow with an angle of 25° between the normal to the plane and the flow direction. Dye particles passing through the light sheet revealed the patterns of higher dye concentration. This method is called laser-induced fluorescence (LIF). Photography and video cameras look perpendicularly at

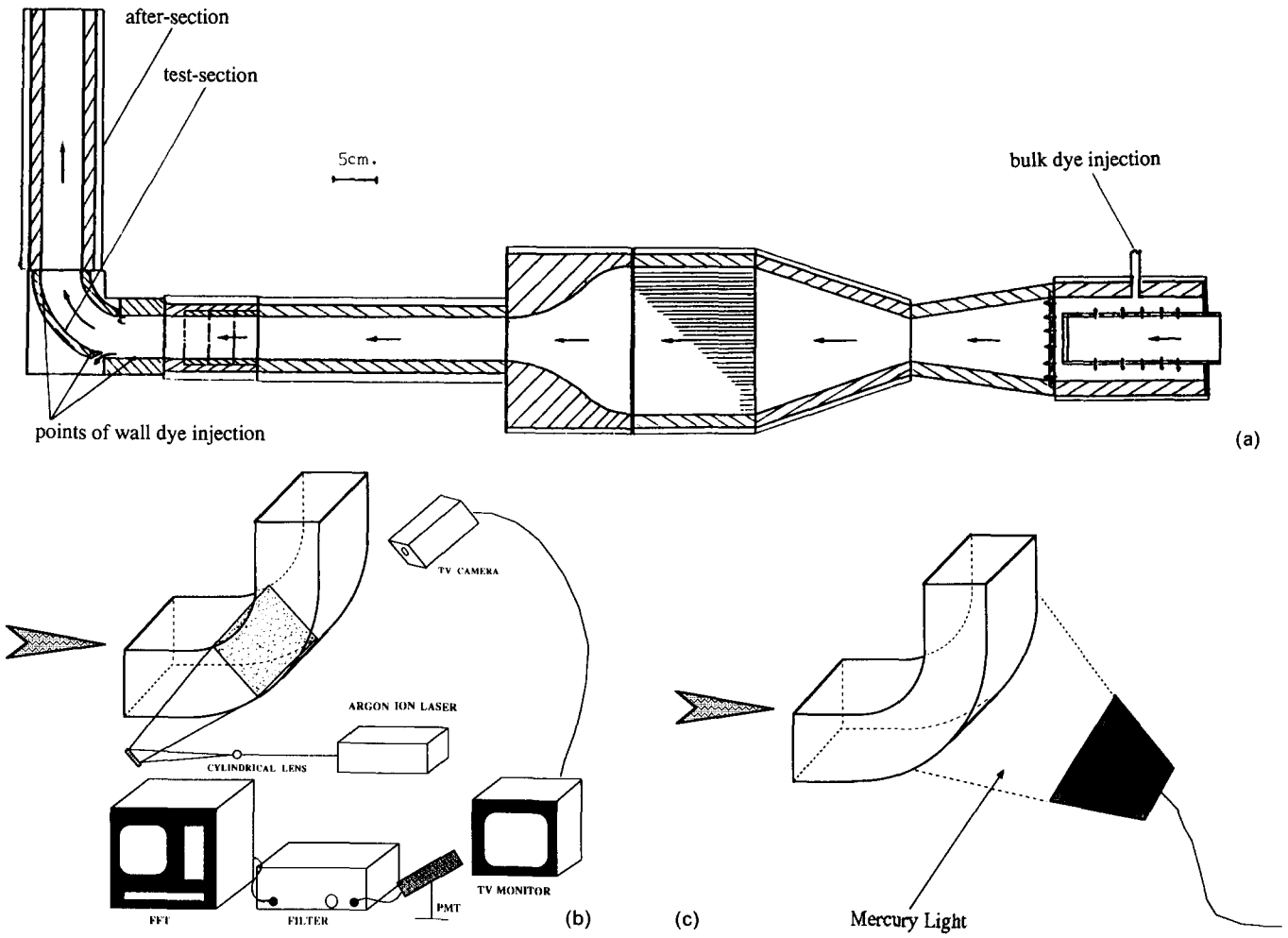

Figure 1 (a) Schematics of water tunnel, (b) LIF arrangement, (c) Back visualization

Notation

G_θ	Görtler number, defined with momentum thickness as typical length
U	Freestream velocity
R	Curvature radius of the streamline or the concave wall
Re	Reynolds number
x	Distance from the leading edge
θ	Momentum thickness of the boundary layer
ν	Kinematic viscosity
α	Angle on the concave wall from the leading edge

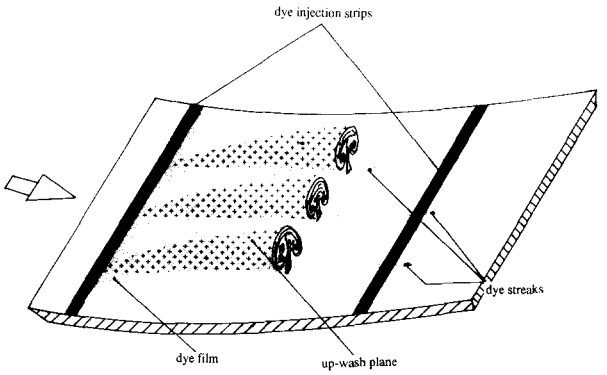

Figure 2 Schematic diagram of roll-formation process

the light sheet (Figure 1b). Oscillation of the interface plane (upwash) between two neighboring rolls was studied using an optical technique. In this technique, fluorescein was injected on the wall (wall-injection method), which was concentrated on the upwash plane. The image of this plane was formed on a T.V. monitor by a video camera. This image was then focused on the pinhole of a photomultiplier tube (PMT). The output signal of the PMT was filtered, amplified, and passed to a fast Fourier transform (FFT) signal anayzer (Figure 1b). Temporal variation of fluorescein concentration on the image of the interface plane followed the dynamics of the rolls' oscillation.

Results and discussion

Roll formation was observed by both wall and bulk dye injection techniques along with back and LIF visualizations.

In back visualization, dye was injected on the wall (wall injection), and visualization was concentrated only on the concave wall looked at from behind (Figure 1c). The dye injected on the wall at 11° (1.9 cm) downstream of the leading edge formed a thin film next to the concave wall. In a short distance downstream of the point of injection, the film started to lose its uniformity by forming longitudinal streaks of high dye concentration and regions where no dye was present (Figure 2). Parallel to the process of streak forming, side views of the test section showed an outflow of a very thin dye layer emerging from the test wall along the dye streaks. The height of the dye layer increased in the flow direction. Proceeding downstream, the outer edge of the layer started to oscillate from side to side while the base of the layer (in contact with the concave wall) stayed fixed. However, further downstream (equivalent to higher Görtler numbers) the base of the outflowing layer also started to wander laterally. The distance from the leading edge to the point where the dye streaks are fully developed is related to the critical length of instability, which was seen to depend on the mean flow velocity.

We attribute formation of dye streaks to the effect of Görtler rolls on the wall. Under action of the counterrotating streamwise rolls, dye is collected from the dye film at spanwise locations where the transverse velocity components of the two neighboring rolls point away from each other and is concentrated where the velocity vectors point toward each other. At the same time, fluid from outside the boundary layer flows downward and replaces the fluid that migrated to the dye concentration zones, and fluid particles that were concentrated along the streaks are forced to flow away from the wall. Thus the dye layer emerging from the wall represents the upwash plane separating two neighboring rolls.

Although back visualization demonstrates the effect of roll activity on the wall, it reveals no information corresponding to the inner structure or the dynamics of the rolls. For this purpose, we used the LIF with wall and bulk dye injection.

By injecting dye on the wall surface (no bulk injection), we observed evolution of the rolls only along an outflow plane (flow coming from the walls seeded with dye). Figure 3 represents schematically three distinct appearances of the outflow plane in the course of roll development. In what follows, we describe observations at a constant freestream velocity ($U = 3.11$ cm/s) for different streamwise distances on the concave test section.

The first observed shape corresponds to when the dye film is still in the process of streak forming ($\alpha \cong 40°$). Under the upwash action of rolls, dye concentrated on the streaks leaves the wall surface and forms a type of "spike" standing out from the wall. At this state, the destabilizing effect is weak and not amplified enough to trigger rolls of a well-defined form capable of being resolved internally by visualization. The pair of rolls looks like a bump and stays attached to the concave wall.

In the second stage when the destabilizing mechanism has strengthened its effect, a ball-shaped concentration of dye appears at the top of the spike, giving it a half-dumbbell shape ($\alpha \cong 60°$). In this state of development, the downflow activity near the boundary-layer edge is stronger than in the previous stage, thus the transverse vortex lines are stretched and bent downward. However, at a higher level of amplification ($\alpha \cong 80°$), the ball-shaped concentration of dye is stretched transversely and forms a mushroom-shaped contour of the rolls pair. Though we describe the process of roll formation in three steps (for the sake of clarity), we by no means suggest they represent distinct physical stages of rolls formation or higher modes of instability. Recent smoke visualization results of Ito[9,10] in wind tunnel and hydrogen bubble visualization results of Sabzvari and Crane[11] have shown the same configuration of the Görtler rolls. However, our visualization results reveal finer inner structures of the rolls.

At higher Görtler numbers ($\alpha > 80°$), the extended flanks of the mushroom roll up and form the low-speed cores of Görtler rolls.

Dye injected on the wall marks the low-speed fluid particles adjacent to the wall that are upwashed away from it (due to instability) and are then forced downward (due to instability) at a different spanwise location to form the contour of the rolls. This visualization, however, does not reveal the fine and active structure that exists inside the Görtler rolls.

We have used simultaneous bulk and wall dye injection coupled with LIF to visualize the inner structure of the rolls. Görtler rolls generated on the concave test section while carrying dye injected on the wall and in the bulk flow enter into the straight after-section, which immediately follows the concave test section. In the after-section, the (centrifugal) destabilizing mechanism is relaxed, and the rolls undergo a milder growth due to viscous diffusion of vorticity only. We have followed a pair of rolls along a distance of 20.5 cm from exit of the concave test section and visualized them at different

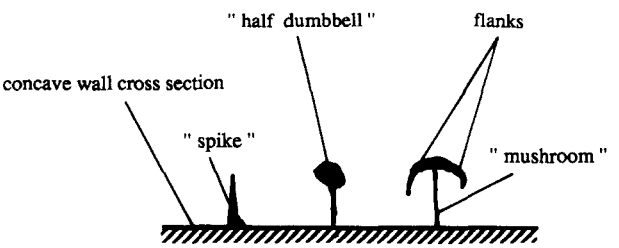

Figure 3 Three distinct appearances of upflow interface between two neighboring rolls

stations by LIF. Figure 4 shows the result of this visualization. In this series of photographs, the vertical bright line (stem of the mushroom) represents the fluid pumped from the wall, whereas less bright streamlines show the path of fluid particles that are marked (by dye) upstream of the test section and are brought to a rotating motion due to the rolls action. In the photographs, it can also be seen that the boundary-layer thickness above the rolls is thicker in the outflow interface compared to the inflow region. When the rolls have grown enough, their centers move away from the wall. This shift of center brings the zone of major roll activity as well as the high shear region far from the wall. This fact can have a major impact on the heat transfer and skin friction characteristics of the flow.

Roll's dynamics and velocity distribution

Once the Görtler rolls have developed in the boundary layer on the concave wall, they undergo an amplification in the downstream direction.

The Görtler number and thus the state of instability get amplified along the flow ($G \propto \alpha^{3/4}$), as is demonstrated by LIF (wall) visualization. For a constant freestream velocity of $U = 3.48$ cm/s, the Görtler number at the exit is calculated as $G_\theta = 5.16$ (the theoretical critical value of G_θ after Görtler's linear stability analysis is 0.58). This estimation is taken under the hypothesis that "the curvature of the streamlines" is equal to $1/R$.* The rolls are then followed in the after-section, where the effect of curvature is relaxed, but the boundary layer and, along with it, the rolls continue to grow. In other words, from the test-section exit on, the Görtler number does not measure the state of amplification of the rolls any more, but it is the Reynolds number that should be considered as the corresponding parameter. Hence to compare the state of the rolls at any distance downstream from the test-section exit with reference to that at the exit plane (end of amplification under Görtler instability effect), one can define a relative Reynolds number as parameter.

We define parameter r as:

$$r = \frac{\mathrm{Re}}{\mathrm{Re}_{\mathrm{exit}}} \tag{2}$$

where Re represents Reynolds number at any distance from the leading edge, and $\mathrm{Re}_{\mathrm{exit}}$ represents Reynolds number at the exit plane. Both Reynolds numbers are calculated based on the boundary-layer momentum thickness θ, developed from the leading edge of the concave wall. Hence

$$r = \frac{\mathrm{Re}}{\mathrm{Re}_{\mathrm{exit}}} = \left(\frac{U\theta}{\nu}\right) \Big/ \left(\frac{U\theta_{\mathrm{exit}}}{\nu}\right) = \left(\frac{x}{x_{\mathrm{exit}}}\right)^{1/2} \tag{3}$$

Indeed, from the point where the rolls enter the after-section, one is faced with the problem of streamwise rolls (no matter from what origin) close to a solid wall evolving with a boundary layer under viscous diffusion from the wall. There is a closer analogy between this flow and, for example, transitional and turbulent boundary layers where streamwise counterrotating rolls develop near the wall; the present situation has the advantage that Görtler rolls are quite regular and steady (compared to transitional and turbulent flows where the rolls are intermittent). This is also the case in many practical situations where rolls are generated in highly concave regions of short extension and then emerge and evolve in straight regions.

In Figure 4, the rolls are identified based on the r parameter defined in Eq. (2).

Görtler rolls shortly downstream of their generation are completely stationary in space (on the concave wall). However, by increasing the Görtler number, the upflow plane between two neighboring rolls starts to oscillate around its stationary position while keeping its points of contact with the concave wall fixed. This situation can be considered the second mode of instability. Oscillation around the first mode is complicated by side movements of the mushroom flanks in phase with the mushroom stem oscillation.

We measured the side oscillation of one of the mushroom flanks using the experimental setup as explained in the previous section (LIF, TV camera, and FFT). For each freestream velocity, we obtained and recorded the average oscillation spectrum over 1000 spectra. Figure 7 shows a typical average spectrum. The average spectra showed a peak at a frequency between 0.200 and 0.275 Hz. The amplitude of the peak showed an increase by increasing the freestream velocity up to a certain velocity. Then it decreased with increasing the freestream velocity and eventually disappeared. The disappearance of the peak coincided with the onset of the "jump-and-stay" mode, in which no coherent frequency could be measured. Figure 8(a) shows a plot of the amplitude of the peak versus the freestream velocity, and Figure 8(b) represents the prevailing frequency (non-dimensionalized on the momentum thickness and kinematic viscosity) versus the freestream velocity.

The side oscillations of the interface plane can be interpreted as being due to an unstable transverse profile of the streamwise velocity: Discrete and abrupt injection of dye in the bulk flow forms a sharp dye front, which as it enters into the light sheet, reveals the existence of transverse and vertical gradients of dye concentration. Dye concentration gradient is related to the streamwise velocity gradient. Depending on the time at which the picture of the flow is taken in relation to the moment at which the dye is injected, regions of dye concentration may represent low-speed or high-speed flow regions. In either case, observation of dye concentration at the light plane showed transverse and vertical gradients, which suggested the existence of unstable transverse and vertical profiles of streamwise velocity, that is, $\partial U/\partial z$ and $\partial U/\partial y$. Low-momentum fluid riding above higher-momentum fluid in the core of the rolls (unstable vertical gradient) gives rise to an inflection point in the streamwise velocity profile normal to the wall. This confirms clearly the unstable situation that was also deduced from hot wire velocity scanning in a pair of Görtler rolls by Swearingen and Blackwelder.[12]

Oscillatory motion of the interface plane between two neighboring rolls is also reported by Wortmann[5] in a slightly different description. Wortmann states that asymmetric appearance of the Görtler rolls, when oscillations set in, "could be imagined (to be) caused by secondary streamwise vortices (rolls) with spanwise distances double those of the Görtler vortices (rolls)." We have no experimental evidence of this description. However, in our experiment, we have not applied a permanent perturbation as in the Wortmann case, where the conditions for spatial resonance of modes exist, as was pointed out by Floryan and Saric.[13]

When the oscillatory motion sets in the flow, the pair of rolls loses its symmetry, and the two neighboring rolls change size intermittently. Oscillation of the interface can be viewed as the "leaning" of the rolls.

The problem of the "leaning cells" was addressed by Hall[14] in

* Lack of precision stems from the fact that the curvature of streamlines and the concave wall are not necessarily the same. The structure of the streamlines are very sensitive to the rate of boundary-layer suction on the concave and convex walls in the entry of the test section. These remarks apply also to the exit of the curved section, where elbow effects and/or flow separation modify locally the curvature in this region and eventually produce a streamline curvature even on the flat region not far from the exit.

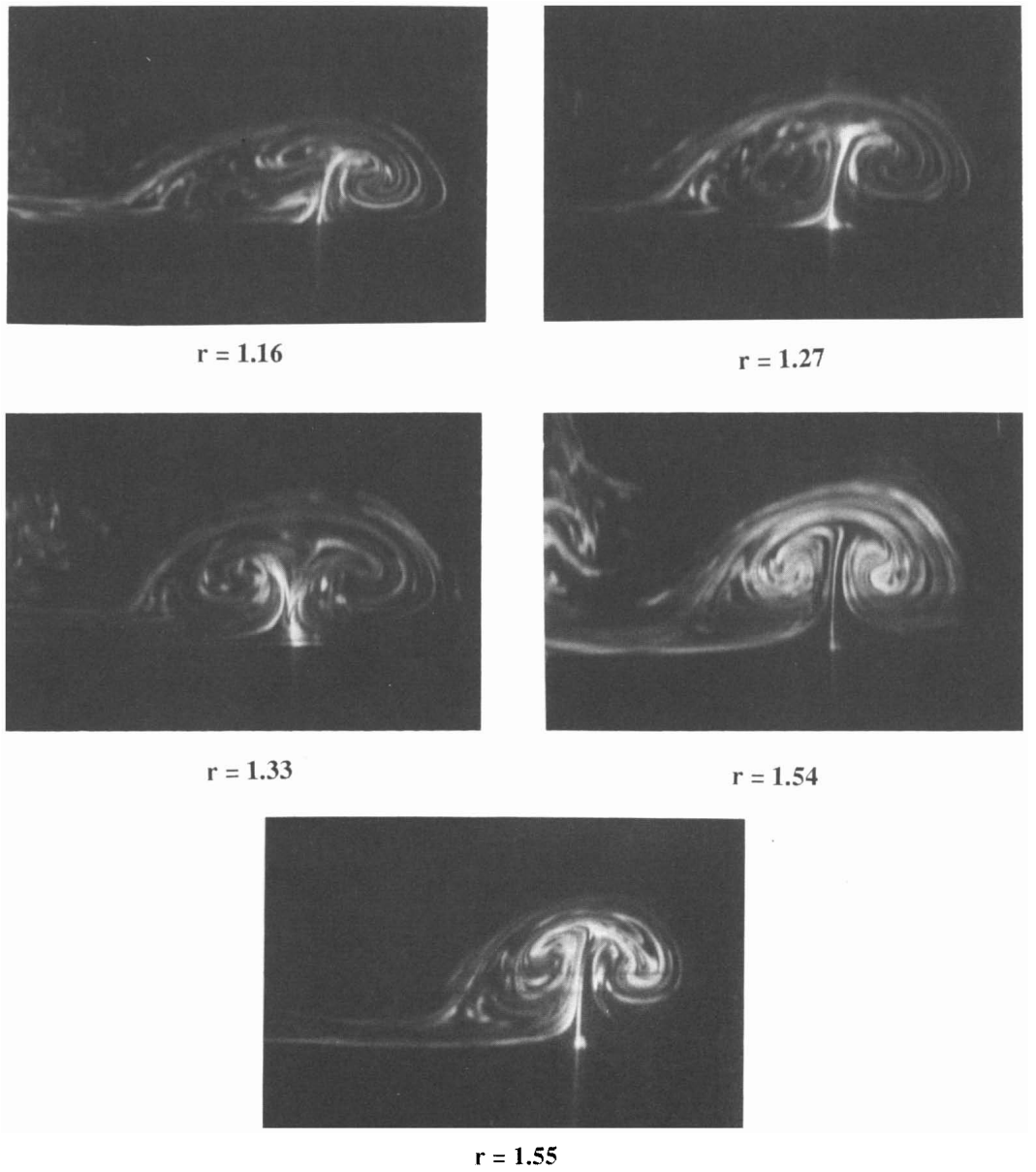

Figure 4 LIF photographs showing a pair of Görtler rolls in the straight after-section at different distances from the test-section exit; U=3.48 cm/s and Görtler number at the test-section exit is G_θ=5.16

a nonlinear analysis of evolution of Görtler rolls in a nonparallel boundary layer. By manipulating the initial conditions of the disturbances (in the analysis), a pair of leaning cells was produced. However, the cells become vertical downstream of the flow, according to Hall, so that the experimental observation of these cells over any reasonable length scale is not to be expected. Winoto and Crane[15] also attributed the larger scatter in their measurement of the streamwise component of the perturbation velocity at the upwash plane to a low-frequency (<0.5 Hz) unsteadiness. They found it consistent with the spanwise wandering of the rolls over a distance considerably less than the rolls' wavelength. Wandering was also reported by Bippes.[6] However, the oscillation we have observed here occurs before the onset of the wandering motion. Oscillations were also predicted by Aihara[16] in the context of the existence of imaginary roots in the dispersion relation. From this analysis, it is not yet evident if these oscillations correspond to the travelling waves (spanwise wandering) or the stationary waves. Analysis of this behavior and comparison with experimental results are in progress.

Higher amplification of the aforementioned state results in an alternating rapid jump of flanks from one side to another with a long residence time at each side (the jump-and-stay motion). This interesting steady behavior is being further studied. Figure 5 represents a typical jump-and-stay motion of a pair of rolls visualized only by wall dye injection and LIF to keep side motions easy to follow. If the velocity is increased further, the jumps of the mushroom flanks become so profound that the interface plane of the rolls bends to the sides and so bring the rolls' centers close to the wall, hence causing drastic changes in the transfer characteristics of the boundary layer. Figure 6 shows such a situation. Winoto and Crane[15] also refer to this jump-and-stay motion but in the context of the meandering motion. They displayed the analogue output from the frequency tracker on a chart recorder and observed a "step-like appearance of $u(t)$ records (which) suggested the existence of two

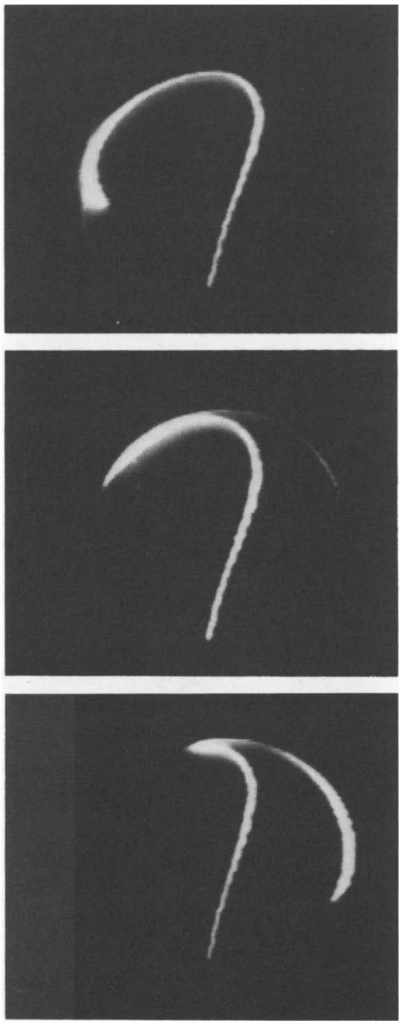

Figure 5 Oscillation of Görtler rolls (LIF with wall dye injection)

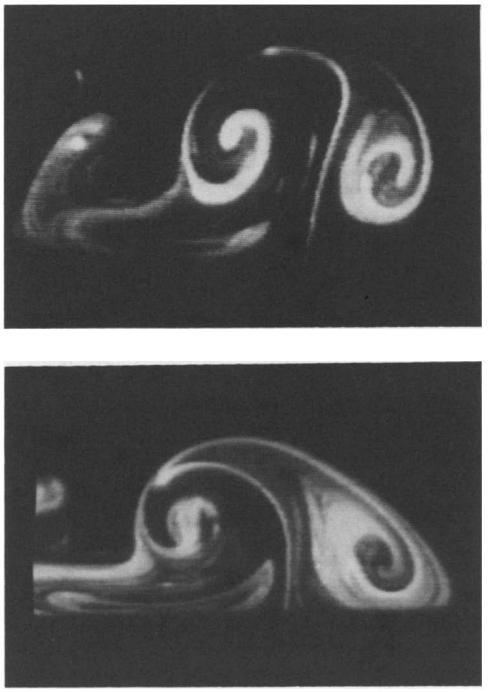

Figure 6 Görtler rolls touch the wall

or three quasi-steady vortex z (spanwise) positions with rapid switching between them."

Spanwise wandering of the rolls, in our experiment, appears as a highly amplified state of the jump-and-stay mode. In this mode, the interface plane of the rolls sharply deforms at a region very close to the wall while it wanders laterally.

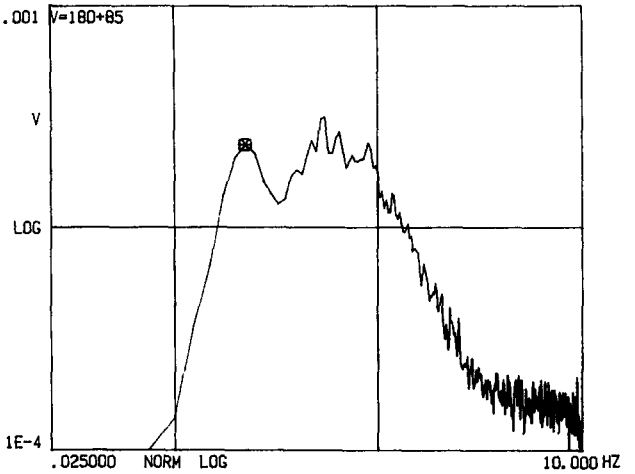

Figure 7 Fourier spectrum of the oscillations for U=2.84 cm/s

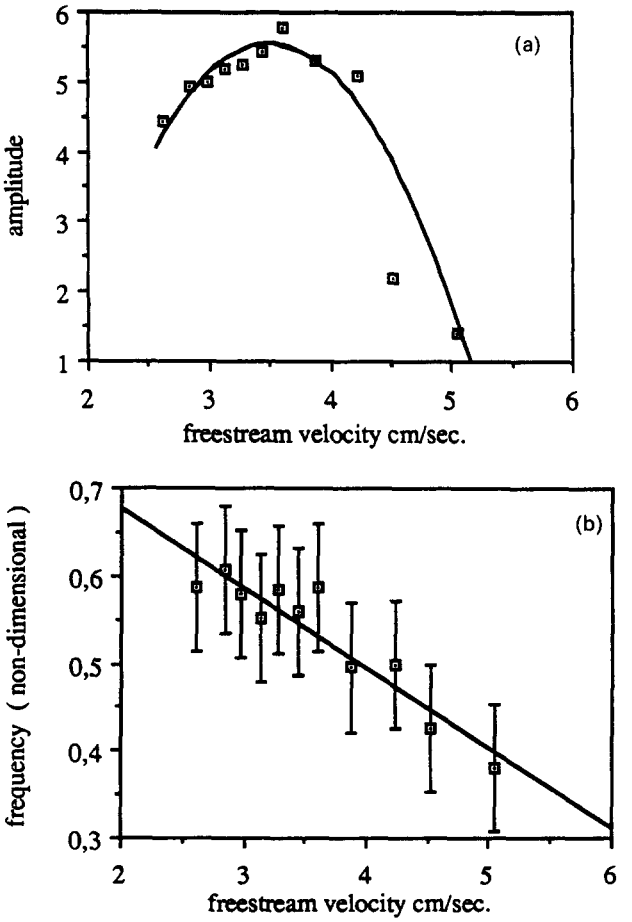

Figure 8 (a) Amplitude of the spectrum peak of the oscillations (b) Nondimensional frequency of the oscillations versus the freestream velocity

Still, at much higher Görtler numbers ($G_\theta > 7$ at the exit of the test section) when the flow is turbulent, LIF visualization shows the rolls, though distorted keep their general shape and appear intermittently in their original spanwise position of initial appearance. At this last state, the rolls very much resemble the structures that Barlow and Johnston stated "seem to appear randomly in space and time at the distinct out-flow regions."[17]

Concluding remarks

A pair of streamwise Görtler rolls is generated in the concave test section owing to centrifugal instability. The rolls are then directed to a straight section where the destabilizing mechanism is relaxed. Our principal observations can be summarized as follows:

1. The rolls are generated near the surface of the concave wall, but their cores gradually move off the wall as the Görtler number grows larger.
2. An oscillatory motion of the stem and flanks first appears at higher Görtler numbers. The oscillatory motion is then followed by a "jump-and-stay motion" of the flanks and roll deformation. This mode is being further explored.
3. Under the oscillatory motion, the rolls bend to the sides, and when the motion is profound enough, they touch the wall. This behavior can affect the heat transfer and skin friction characteristics of the boundary layer.
4. The rolls keep their general appearance (but distorted) even when the boundary layer is turbulent.

Acknowledgments

We thank M. Clément for his enthusiastic participation in this project. We want also to present our acknowledgments to M. Lux and the staff of the Prototype Center of CNRS (Meudon-Bellevue) for their technical assistance.

This work was supported by the Ministere de la Recherche et Technologie (France) under Grant N° 85 P 1471.

References

1 Kottke, V. Taylor-Görtler vortices and their effect on heat and mass transfer. Proc. Eighth Int. Heat Transfer Conf., 1986, San Francisco, 1139–1144

2 McCormack, P. D., Welker, H., and Kelher, M. Taylor-Görtler vortices and their effect on heat transfer. *J. Heat Transfer*, 1970, **92**, 101–112

3 Peerhossaini, H. The Görtler rolls. ESPCI Report R-86-24, 1985

4 Peerhossaini, H. On the subject of Görtler vortex. *Cellular Structures in Instabilities*, ed. J. E. Wesfreid and S. Zaleski. Springer-Verlag, Berlin, 1984

5 Wortmann, F. X. Visualization of transition. *J. Fluid Mech.*, 1969, **39**, 473–480

6 Bippes, H. Experimental study of laminar turbulent transition of a concave wall in a parallel flow. NACA TM 75243, 1978

7 Swearingen, J. D. and Blackwelder, R. F. Parameters controlling the spacing of streamwise vortices on a concave wall. AIAA Paper No. 83-0380, 1983

8 Peerhossaini, H., Clement, M., Wesfreid, J. E. Boundary layer instability due to Görtler rolls. ESPCI Report RS-85-71, 1985

9 Ito, A. The generation and breakdown of longitudinal vortices along a concave wall. *J. Japan Soc. Aero. Space Sciences*, 1980, **28**, 327–333 (in Japanese)

10 Ito, A. Breakdown structure of longitudinal vortices along a concave wall. *J. Japan Soc. Aero. Space Sciences*, 1985, **33**, 166–172 (in Japanese)

11 Sabzvari, J. and Crane, R. I. Effect of Görtler vortices on transitional boundary layers. *Three-Dimensional Flow Phenomena in Fluid Machinery*, ed. A. Hamed *et al.* ASME publication, New York, 1985

12 Swearingen, J. D. and Blackwelder, R. F. Breakdown of streamwise vortices near a wall. *Structure of Complex Turbulent Shear Flows; IUTAM Symp. 1982*, ed. R. Dumas and L. Fulachier. Springer-Verlag, New York, 1982

13 Floryan, J. M. and Saric, W. S. Wavelength selection and growth of Görtler vortex. *AIAA Journal*, 1984, **22**, 1529–1532

14 Hall, P. On the nonlinear evolution of Görtler vortices in nonparallel boundary layers. *IMA J. of Applied Math.*, 1982, **29**, 173–196

15 Winoto, S. H. and Crane, R. I. Vortex structure in laminar boundary layers on a concave wall. *Int. J. Heat and Fluid Flow*, 1980, **2**, 221–231

16 Aihara, Y. Nonlinear analysis of Görtler vortices. *Phy. Fluids*, 1976, **19**, 1655–1610

17 Barlow, R. S. and Johnston, J. P. Structure of turbulent boundary layers in a concave surface. Stanford Report MD-47 and Roll cells in concave turbulent boundary flows, a 16-mm color movie